



PERGAMON

Available online at www.sciencedirect.com

SCIENCE @ DIRECT®

Planetary and Space Science 51 (2003) 9–17

Planetary
and
Space Sciencewww.elsevier.com/locate/pss

Ultraviolet and infrared spectrum of C_6H_2 revisited and vapor pressure curve in Titan's atmosphere

F. Shindo^{a,*}, Y. Benilan^a, J.-C. Guillemin^b, P. Chaquin^c, A. Jolly^a, F. Raulin^a^aLISA, UMR 7583, Universités Paris 7 & 12, 61 avenue du Général de Gaulle, 94010 Créteil Cedex, France^bLSAB (Laboratoire de Synthèse et Activation de Biomolécules), UMR 6052 CNRS, ENSCR, Avenue du Général Leclerc, 35700 Rennes Cedex, France^cLaboratoire de Chimie Théorique, Université Paris VI, 4 place Jussieu, 75005 Paris, France

Received 16 April 2002; received in revised form 26 August 2002; accepted 26 September 2002

Abstract

The presence of the linear molecules called polyynes, ($C_{2n}H_2$, $n > 2$), in Titan's atmosphere is suggested by the signatures of acetylene C_2H_2 and of diacetylene C_4H_2 in Voyager spectra. Both atmospheric simulations and photochemical modelling support polyynes implication in Titan's chemistry as an interface between the gaseous phase and the solid phase visible in aerosols form. However, the detection of polyynes higher than C_4H_2 depends on our ability to determine their spectra in the laboratory under low temperature and pressure conditions. We revisit here spectroscopic investigations on triacetylene, C_6H_2 , since previous UV and IR measurements suffered from great uncertainty, respectively, due to an impurity contribution and saturation effects. We point out the importance of studying a pure sample and we underline the strong temperature dependency of UV absolute absorption coefficients (185–320 nm). In the IR range (220–4300 cm^{-1}), our determination of the absolute intensity of the main bands is 30% higher than previous measurements. For the first time, the vapor pressure law of triacetylene is investigated in a limited temperature range (170–200 K) allowing a calculation of its enthalpy of sublimation. Those results applied to Titan's atmospheric conditions show the possible existence of two condensation regions: one located in the low stratosphere (~ 100 km) and the other in the thermosphere (~ 700 km). The condensation at an altitude of 700 km is consistent with the observation of an upper haze layer. This could imply the presence of a heterogeneous chemistry but also an inhibition of the polyynes formation, not included in available photochemical models.

© 2002 Elsevier Science Ltd. All rights reserved.

Keywords: Titan; Polyynes; Triacetylene; Spectroscopy; Enthalpy; Aerosols

1. Introduction

Titan, the largest moon of the Kronian system, owns a dense atmosphere where methane was the first compound observed (Kuiper, 1944) before Voyager observations highlighted nitrogen as the main constituent (Broadfoot et al., 1979; Strobel, 1982). Voyager observations revealed an atmospheric composition rich in numerous organic constituents, mainly hydrocarbons and nitriles (Hanel et al., 1981; Kunde et al., 1981; Maguire et al., 1981) resulting, respectively, from the photochemistry of methane and nitrogen in upper atmosphere. This complex chemistry is predicted to lead to the unsaturated organic linear molecules

called polyynes (Yung et al., 1984), of general formula $C_{2n}H_2$ ($n = 1, 2, \dots$). But, the only polyyne detected so far in Titan's stratosphere is diacetylene formed by the acetylene photochemistry (Laufer and Bass, 1979; Okabe, 1983). Its presence suggests the existence of heavier polyynes as C_6H_2 or C_8H_2 (Bandy et al., 1992), detected experimentally as end products of diacetylene photolysis (Bandy et al., 1993; Frost et al., 1995). Besides, the formation of heavier polyynes in Titan is strengthened both by the detection of triacetylene and tetracetylene in experimental works simulating Titan's atmosphere (Coll et al., 1999; de Vanssay et al., 1995) and by theoretical modeling of Titan's atmospheric chemistry (Lara et al., 1996; Toublanc et al., 1995). Those results also suggest that polyyne photochemistry may contribute to the production of longer and heavier molecules whose condensation could provide an interface between gaseous and solid phase, visible in haze form at Titan's limbs (Allen et al., 1980; Chassefière and Cabane, 1995). Moreover, polyynes

* Corresponding author. Tel.: +33(0)-1-45-17-15-36; fax: +33(0)-1-45-17-15-60.

E-mail address: shindo@lisa.univ-paris12.fr (F. Shindo).

may also be involved in Giants Planets chemistry since diacetylene signature was identified in ISO (Infrared Space Observatory) spectra of Saturn by [de Graauw et al. \(1997\)](#) and predicted in Jupiter by the photochemical model of [Gladstone et al. \(1996\)](#). However, the observational confirmation of the formation of polyynes heavier than C_4H_2 requires the knowledge of their gaseous spectra, which is still scarce or partial, mainly due to the high instability of such compounds at room temperature. For this reason, we are developing a program called SCOOP (Spectroscopie de Composés Organiques Orientés vers la Planétologie) to determine UV (180–320 nm) and IR (220–4300 cm^{-1}) absolute absorption coefficients of organic compounds predicted in Titan's atmosphere, such as polyynes. In this context, our team led the only studies on absolute spectroscopic characteristics of triacetylene ([Bénilan et al., 1995](#); [Delpech et al., 1994](#)), but those suffered from great uncertainties, which prevent to infer a definite spectrum. These uncertainties were due to the contribution of impurities in the sample and to a saturation effect on the IR measurements. Consequently, we reinvestigate the triacetylene spectrum in this paper from a pure sample, in mid-ultraviolet and infrared wavelength range.

The first section describes our protocol to remove the impurity and obtain a pure C_6H_2 sample, as well as the instrumental set up. In the following section we present our results: we emphasize the changes on the UV spectrum caused by the impurities removal, and we highlight the spectral variations between our measurements at 300 and 233 K. We also report polyynes spectroscopic behavior with the length of the molecular chain. In Section 2 we point out the vapor pressure curve of triacetylene measured between 170 and 200 K. The third section presents our determination of bands positions and intensities in IR wavelength range. In the final section we infer an upper limit of triacetylene mole fraction in Titan's atmosphere and determine its condensation regions.

2. Experimental

The synthesis of triacetylene is described in [Delpech et al. \(1994\)](#). As reported by [Bénilan et al. \(1995\)](#), the resulting compound is in fact a mixture of triacetylene and one of its chemical precursor (C_6H_3Cl). Obviously, the precursor contribution affects our knowledge of the triacetylene pressure, required to measure absolute absorption. But, another effect changes dramatically the mid-UV spectrum: the structures of a C_6H_3Cl allowed transition overlap the structures of the C_6H_2 forbidden transition standing in the 200–300 nm wavelength range. Therefore, we focused our efforts on the separation of these two compounds.

2.1. Studied gaseous sample preparation

The specifications of the SIPAT experience (see [Bruston et al., 1991](#)) allow the distillation of a mixture with the

vapor pressure of each compound. Our sample is condensed at a “cold spot” (a glass container immersed in a liquid nitrogen bath), which we can regulate the temperature. The two compounds have close molecular mass and also close vapor pressure curve so that a fine distillation had to be performed. Observing the spectrum of the vaporized mixture, we found that the evaporation of the pollutant seems to be almost inhibited for a cold spot temperature of $-82^\circ C$. At this temperature, the evaporated part is collecting in a trap bathing in liquid nitrogen. The composition of this purified sample is then checked by GC-MS analysis: no traces of C_6H_3Cl were detected using such protocol.

2.2. Instrumental and experimental specifications

We used the SIPAT spectrometer to investigate the ultraviolet spectrum in the range 185–320 nm. We measured the absolute absorption coefficients at 300 and 233 K; and at those temperatures, the pressure was respectively 2×10^{-2} mb and 9×10^{-3} mb. Although we measured spectra at our higher resolution of 0.2 Å, no structural changes appeared at a resolution of 1 Å. This is probably due to a strong predissociation of the electronic bands. For each temperature, the final spectrum is an average of five scans with 3 points/Å and an integration time of 1 s per point. The wavelength calibration of the SIPAT spectrometer is based on a comparison between theoretical and experimental rotational lines of the Schumann–Runge bands system of molecular oxygen in the range 190–196 nm. The positions of rotational lines are taken from the HITRAN database and allow us to construct a synthetic spectrum of O_2 with the higher resolution reached by SIPAT (0.2 Å), taking into account of the spectrometer instrumental profile and the predissociation linewidth.

Infrared spectra (from 220 to 4300 cm^{-1}) were obtained by an IRTF spectrometer (Perkin-Elmer 1710). It was equipped with a cell of 10 cm pathlength to proceed in the pressure range 0.1–10 mb. We have avoided bigger pressure because of the compound instability. Minor bands were measured with a cell of 10 m pathlength. In this case, the required pressures could reach values around 10^{-2} mb.

3. Results

3.1. Mid-UV spectrum

We present here the absolute absorption coefficients of pure C_6H_2 sample in the range 185–300 nm (Fig. 1), obtained, respectively, at 300 and 233 K. In Fig. 1a, we distinguish a segment of the allowed transition $^1\Sigma_u^+ \leftarrow ^1\Sigma_g^+$ shared by all the polyynes ([Haik and Jungen, 1979](#); [Kloster-Jensen et al., 1974](#)). Between 200 and 320 nm (Fig. 1b), the structures are due to an overlap of two forbidden transitions ($^1\Sigma_u^- \leftarrow ^1\Sigma_g^+$ and $^1\Delta_u \leftarrow ^1\Sigma_g^+$). Those are 10^3 times weaker than the allowed transition. The previous determination of

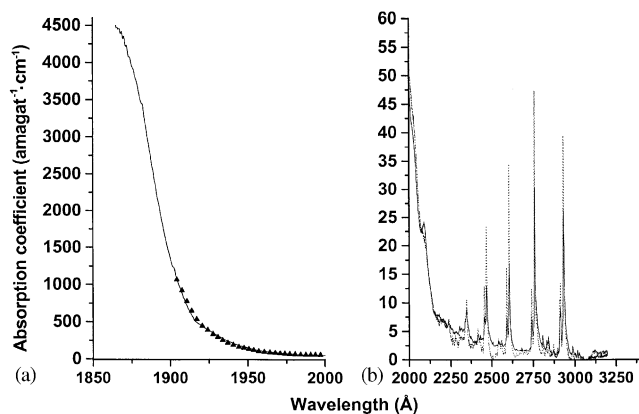


Fig. 1. UV spectrum of C_6H_2 with a resolution of 1 \AA . At 300 K, the sample pressure was $2 \times 10^{-2} \text{ mb}$ (straight line). At 233 K, the sample pressure was $9 \times 10^{-3} \text{ mb}$ and the absolute absorption coefficients are figured either by triangle symbols (left) or by a dotted line (right). (a) The rise of the allowed transition ${}^1\Sigma_u^+ \leftarrow {}^1\Sigma_g^+$ from 185 (190 nm for 233 K) to 200 nm. (b) The forbidden transitions ${}^1\Sigma_u^- \leftarrow {}^1\Sigma_g^+$ and ${}^1\Delta_u \leftarrow {}^1\Sigma_g^+$ complex from 200 to 320 nm.

absolute C_6H_2 ultraviolet spectrum (Bénilan et al., 1995) was uncertain because of the presence of a chlorinated compound at a mixing ratio of 0.1. For such concentration, the impurity spectrum presents absorption features as strong as those of triacetylene. This forced the authors to subtract the pollutant contribution from their measurements to retrieve the C_6H_2 spectrum. Comparing the values reported in Table 1, the two previous works (Kloster-Jensen et al., 1974; Bénilan et al., 1995) present UV absolute absorption coefficients significantly greater than ours. Figs. 2a and b can provide an explanation for these differences: the difference between the previous UV spectra and the present spectrum clearly matches the UV spectrum of the impurity.

The spectrum structure and intensity are very temperature sensitive (Fig. 3). The main temperature dependences are displayed in Fig. 4, by depicting the effects on two characteristic examples of a cold band (8_0^1 and 8_0^2) and a hot band. The cold bands undergo an increase of their maximum absorption coefficient and a narrowing of their FWHM. At the opposite, the hot bands decrease or even disappear as illustrating in Fig. 4b. Indeed, according to Boltzmann distribution, excited vibrational levels are less populated and so hot bands decrease with a temperature drop. This effect also leads the continuum level to diminish, since this continuum is due to a superposition of highly excited levels. The absorption coefficient evolution between 300 and 233 K (Fig. 5) is in agreement with the bands identification given by Haink and Jungen (1979), excepted for the two hot bands $2_0^3 8_1^1$ and $2_0^2 8_1^1$ for which a light increase of absorption coefficient is detected. As pointed out by Bénilan et al. (1996), the superposition of cold bands and hot bands due to pre-dissociation could explain the unexpected variation of these two hot bands. Two features at 2338 and 2348 Å seem to behave like cold bands, however they were not previously

assigned (Fig. 3). Following the previous identification pattern, we could assign them to be respectively the $2_0^4 8_0^1$ and $2_0^4 8_0^2$ bands (Fig. 3). A spectroscopic investigation of the allowed transition (150–200 nm) at high resolution is needed to be able to assign all the features observed (Fig. 4b).

As we investigated the entire range of the forbidden transition, we have checked the conservation of the oscillator strength with temperature. Indeed, we found a difference of 0.2% for a surface of $1.7 \times 10^5 \text{ amagat}^{-1} \text{ cm}^{-2}$ corresponding to an oscillator strength of 4.4×10^3 . In addition, we also covered the range 185–200 nm at 300 K (Fig. 1a) to scale the relative intensities of Kloster-Jensen et al. (1974) of the allowed transition system, which spreads down to 150 nm. For this transition, we retrieved an oscillator strength equal to 1.49 ± 0.3 . This value is two times weaker than the one deduced from Bénilan et al. (1995) spectrum. But, taking into account of C_4H_2 (Fahr and Nayak, 1994) and C_2H_2 (Smith et al., 1991) UV spectra, we remark a linear rise of the polyynes oscillator strength vs. the length of the polyynes chain (see Fig. 5). Experimental points are in accordance with the prediction of this linearity by theoretical calculations (based on the ZINDO method (Ridley and Zerner, 1973) with the VSTO-6G (5d,7f) basis set).

3.2. Vapor pressure curve

As the pressure in the cell is directly linked to the vapor pressure of the compound at the cold point, with our pure sample of C_6H_2 we had the opportunity to determine its vapor pressure vs. temperature. Since we have an equilibrium between the flux created at the cold point temperature (T_{cs}) and the flux inside the cell which is at room temperature (T_{cell}), the vapor pressure P_{vap} is related to the measured cell pressure P_{cell} by the expression

$$P_{vap} = P_{cell} \sqrt{\frac{T_{cs}}{T_{cell}}}. \quad (1)$$

We were able to investigate only a limited temperature range between 170 and 200 K, due to the pressure sensor sensitivity (about 10^{-5} mb) and to the small amount of sample available. To extrapolate our results to the lower temperatures standing in Titan's lower atmosphere, we use the Dupr e equation (2). Indeed, Smith (1999) applied different extrapolations to the vapor pressure curve of acetylene (from 180 down to 70 K), and the Dupr e formulation gives the best fit at low temperatures, even if that extrapolation overestimates vapor pressures at 90 K by one magnitude. Consequently, the relation between the pressure P (in mb) and the temperature T (in Kelvin) is given by

$$\ln P = \alpha - \frac{\beta}{T}. \quad (2)$$

The two parameters α and β are determined from a least square fit to our experimental data. Extrapolation and experimental vapor pressure curves are presented in Fig. 6.

Table 1
UV absorption coefficients of various features measured in this work and in previous works

Wavelength (Å)	Identification ^a	Calibrated intensities ^b	Previous ^c Absorption coefficient (amagat ⁻¹ cm ⁻¹)	Absorption coefficient at 300 K from this work (amagat ⁻¹ cm ⁻¹)	Absorption coefficient at 233 K from this work (amagat ⁻¹ cm ⁻¹)
3017	8 ₀ ⁰	0.8		1.7	1.1
2988	8 ₁ ¹	1.1	3.4	2.4	1.3
2933	8 ₀ ¹	15.8	22	26	39.6
2914	8 ₀ ²	5.7	9	9.3	13.4
2874		1.6	3.3	1.8	2.9
2843		2.9	5.5	3.8	4.1
2808	2 ₀ ¹ 8 ₀ ¹	3.8	6.7	4.3	2.8
2758	2 ₀ ¹ 8 ₀ ¹	29.5	45.2	30.4	47.4
2742	2 ₀ ¹ 8 ₀ ²	12.6	19.5	7.7	12.3
2682		5	8	2	2.2
2670		3.8	6.4	1.7	1.2
2649	2 ₀ ² 8 ₁ ¹	4.5	8	1.9	1
2606	2 ₀ ² 8 ₀ ¹	24.2	40.6	17	33.5
2592	2 ₀ ² 8 ₀ ¹	12.5	19	7.4	16.2
2562		4.7	7.9	3	3.7
2543		4	7.5	3.1	3.7
2508	2 ₀ ³ 8 ₁ ¹	3.9	6.9	3	0.7
2469	2 ₀ ³ 8 ₀ ¹	12.9	22.3	12.9	23.4
2457	2 ₀ ³ 8 ₀ ²	8.1	12.2	7.5	12.7
2432		4	6.9	4.2	4.3
2417		4	6.5	4.4	5.3
2348		5.5	10.1	9	10.5
2338				6.9	7.2
2305		2.7	5.1	5.9	7.2
2237		2.6	5.8	5	7.2
2092		28.1	54.5	23.8	21
2030		35.1	57.6	38.5	41
2013		42.2	58.3	42.6	47
1996		49.2		50.6	54.3
1863		4446.9		4579.4	
1850		4750.3			
1831		5399			
1793		5236			
1761		3387.9			
1727		2703			
1665		944.5			
1596		335.8			

^aFrom Haink and Jungen (1979).

^bThe relative intensities from Kloster-Jensen et al. (1974) scaled to our spectrum by a least-square fit.

^cFrom Bénilan et al. (1995).

From the pressure expression (2), we derive an enthalpy of sublimation equal to $\beta R = 42 \text{ kJ mol}^{-1}$.

3.3. Infrared band intensities

Among the 13 fundamental modes of vibrations of triacetylene only six are infrared active: three modes have Σ_u^+ symmetry and the three others have Π_u symmetry (two times degenerated) (Bjarnov et al., 1974). In the investigated spectral domain (220–4300 cm^{-1}), three intense bands merge from the spectrum corresponding to the ν_{11} mode (Haas et al., 1994a), the bending combination modes $\nu_8 + \nu_{11}$

(Mc Naughton and Bruget, 1991), and the ν_5 mode (Matsumara et al., 1993). The other infrared active modes are also observed with the 10 m pathlength cell, but with a 100 times weaker intensity. For all the detected bands, we determine the absolute intensity S_v given by

$$S_v = \frac{1}{pl} \int_{\text{band}} (I/I_0) d\bar{\nu}, \quad (3)$$

where p is the pressure in the cell, l the pathlength, and I/I_0 the transmission. This expression is valid unless the band is saturated: in this case, the band surface is no more linearly related to the pressure of the compound. Consequently, several spectra of different pressure of triacetylene were mea-

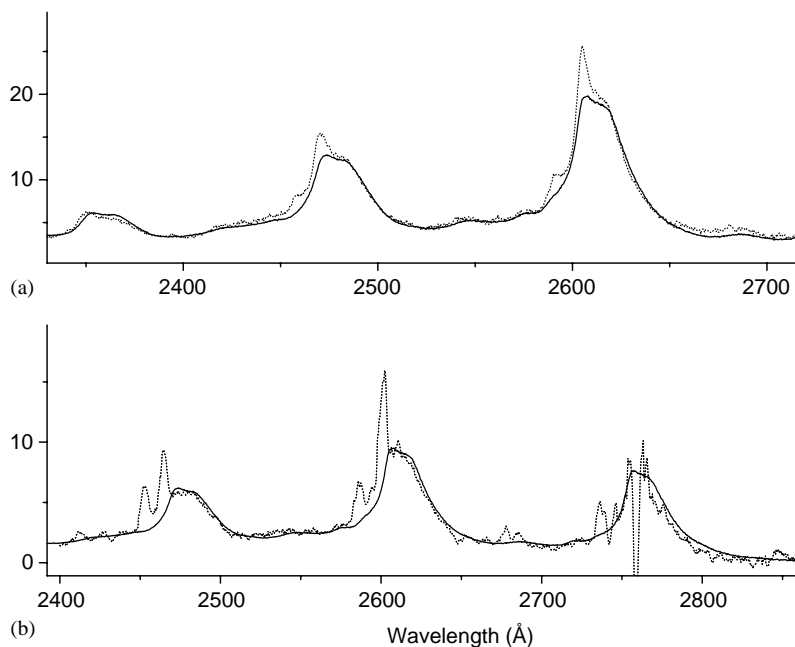


Fig. 2. Difference between the two previous C_6H_2 UV spectra and our spectrum. In straight line we figure the UV spectrum of C_6H_3Cl . (a) In dotted line, the difference between Bénilan et al. (1995) spectrum and our spectrum. (b) Same work on Kloster-Jensen et al. (1974) spectrum.

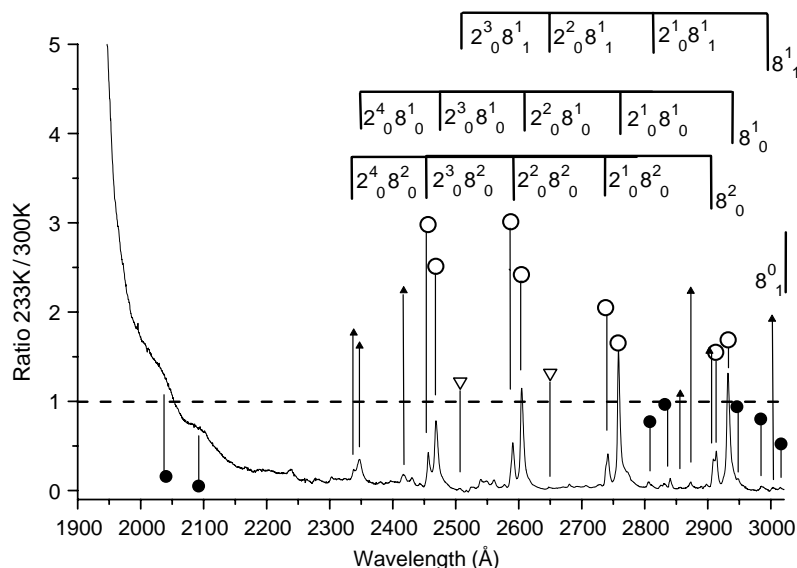


Fig. 3. Ratio of absorption coefficients at 300 and 233 K, corrected from an estimated continuum contribution. Intensities of the cold bands (open circle) are enhanced while hot bands (dark circle) decrease. Non assigned cold bands (black triangle) are also observed between 2300 and 2600 Å. Two hot bands (open triangle) show ratios greater than unity (see text for details).

sured. The resulting band surfaces (in cm^{-1}) vs. the pressure are reported in Fig. 7. For the three main bands, we clearly distinguish a saturation effect above 5 mb, which means that only the points under this pressure have to be taken into account in the calculation of S_v . For those bands, the present results are higher of 30 percent than those of Delpech et al. (1994). Indeed, some of their experimental points fall in the saturated region described above, which led them to underestimate bands absolute intensity. We report the absolute intensities for all the observed bands in Table 2. Unfortunately,

some identified features are too weak to be studied. Finally, some other bands are too close to be separated with our low resolution, and so we indicate S_v for the whole feature.

4. Extrapolation to the Titan's atmosphere

From the spectra of Titan's North Pole, we deduced an upper limit of 4.4×10^{-10} on the mole fraction of C_6H_2 in the low stratosphere (around 100 km), using the method

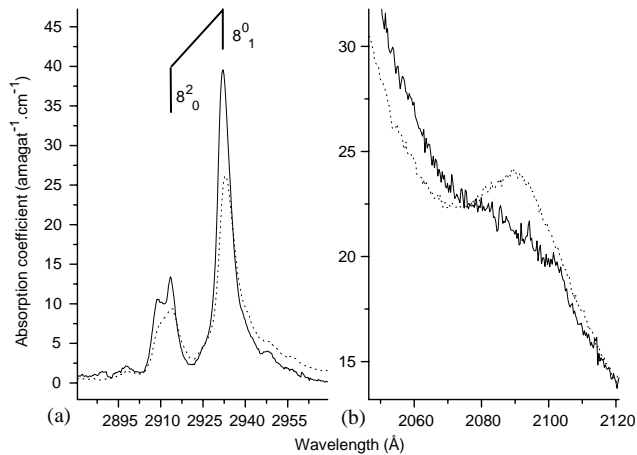


Fig. 4. Effect of the temperature on the spectrum, in dotted line at 300 K and in straight line at 233 K. (a) A cold band exhibits an increase of its maximum intensity and a diminution of its FWHM as the temperature decreases. (b) On the contrary, according to Boltzmann distribution, excited vibrational levels are less populated and so hot bands decrease or vanish when temperature drops off.

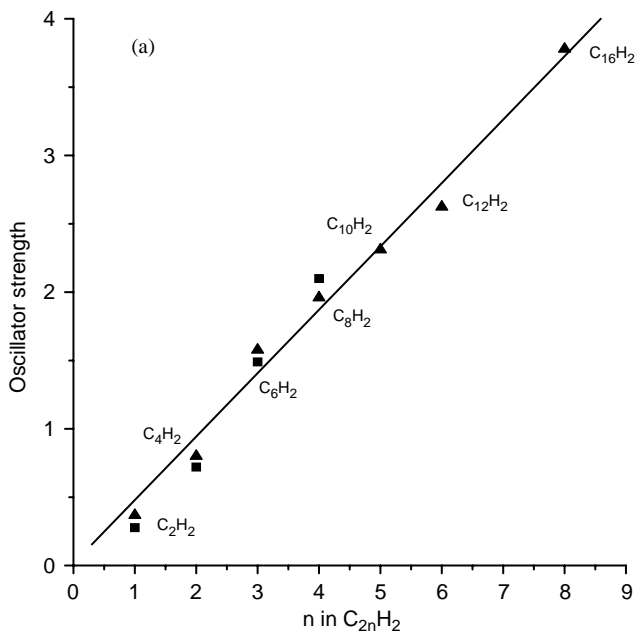


Fig. 5. Polyynes oscillator strength of the ${}^1\Sigma_u^+ \leftarrow X^1\Sigma_g^+$ transition. The measurements (square) and the theoretical predictions (triangle), calibrated by a factor of 0.4, are in accordance and show a linear increase up to $C_{16}H_2$.

proposed by Cerceau et al. (1985). This value is determined from the strongest band of C_6H_2 in the 200–1200 cm^{-1} range, namely the ν_{11} band at 620 cm^{-1} . We do not consider the two other intense bands of triacetylene for this calculation since ν_5 is beyond the wavelength domain of CIRS and of IRIS observations, and $\nu_8 + \nu_{11}$ is totally hidden by the emission features of the major hydrocarbon CH_4 .

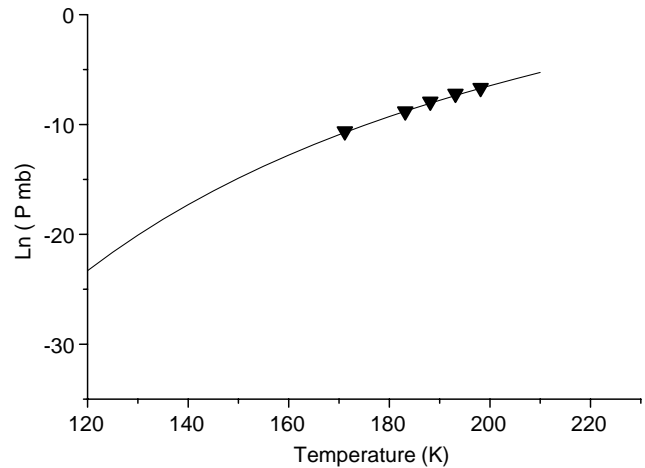


Fig. 6. Experimental vapor pressure curve of C_6H_2 . The measurements (triangle) were performed from 170 to 210 K, and extrapolated to lower temperature using the Dupré equation $\ln(P) = 18.8 - (5053/T)$.

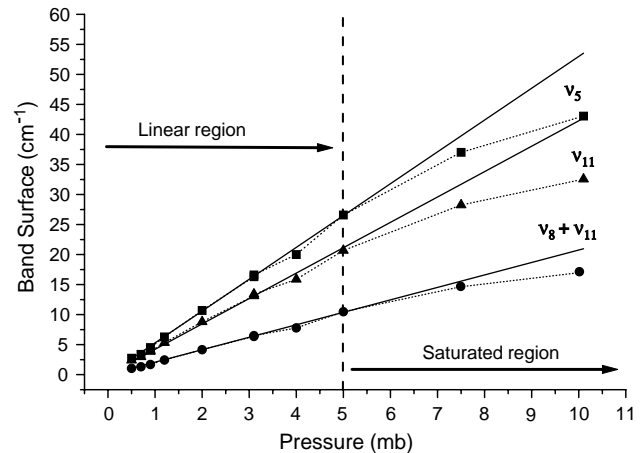


Fig. 7. Band surface versus pressure for the three main bands of C_6H_2 . Band intensities are obtained as the slope of the linear regression divided by the pathlength. This method is not valid anymore in our experiment above 5 mb where saturation occurs.

We report in Fig. 8 the triacetylene vapor pressure profile in Titan's atmosphere, as well as its uncertainty, both deduced from the temperature profile of Lellouch and Hunten (1987). For the vertical profile of C_6H_2 , we consider both the rough approximation of a constant mole fraction through the atmosphere and the triacetylene mixing ratio calculated by the photochemical model of Toubanc et al. (1995), from 400 to 1200 km. The existence of a condensation region is highly sensitive to the temperature uncertainty (see Eq. (2)). A first region can occur at 750 km, in the thermosphere, where the C_6H_2 mixing ratio exhibits a maximum, for a total pressure of 5×10^{-5} mb and a temperature around 115 K. The thickness of this condensation layer would be limited, since below 690 km the C_6H_2 pressure becomes inferior to its vapor pressure inferred from the saturation law, so that triacetylene will re-evaporate. However, the

Table 2
Infrared positions and integrated intensities of triacetylene bands in the 400–4000 cm^{-1} range

Band	Position cm^{-1}	S_{ν} $\text{atm}^{-1} \text{cm}^{-2}$
$\nu_1 + \nu_{11}$	3930	8.0 ± 0.4
$\nu_1 + \nu_{13}$	3432	3.7 ± 0.2
$3\nu_7$	3350	Hidden by ν_5
ν_5	3332 (R)	537 ± 45
	3322 (P)	
$\nu_2 + \nu_7$	3304	Hidden by ν_5
$\nu_3 + \nu_8 + \nu_{11}$	3251 (R)	
	3242 (P)	7.9 ± 0.4
$\nu_1 - \nu_{13}$	3222	
$\nu_3 + \nu_7$	3086	
	3081	1.0 ± 0.1
	3075	
ν_6	2121	6.3 ± 0.3
$\nu_7 + \nu_9$	1588	2.4 ± 0.2
$2\nu_9 + \nu_{11}$	1588	
$2\nu_{11} + \nu_{13}$	1337	1.8 ± 0.2
$\nu_8 + \nu_{11}$	1237 (R)	210 ± 10
	1229 (P)	
$2\nu_{10} + \nu_{11}$	1126	2.4 ± 0.1
ν_7	1123	
	1113	
$\nu_9 + \nu_{12}$	915	< 1
$\nu_{10} + \nu_{11}$	866	2.7 ± 0.1
$\nu_4 + \nu_{13}$	730	4.2 ± 0.2
$\nu_8 + \nu_{13}$	720	
$\nu_{10} + \nu_{13}$	698	18.3 ± 0.9
	690	
ν_{11}	628 (R)	
	622 (Q)	428 ± 25
	617 (P)	
$\nu_9 + \nu_{13}$	595	Hidden by ν_{11}
ν_{12}	444	15.2 ± 0.7

existence of this condensation layer is hypothetical because of temperature and abundance uncertainties. For example, using the temperature profile deduced by Vervack et al. (1999), no condensation is possible at these altitudes. Nevertheless, considering higher polyynes, which would have lower vapor pressure, a haze layer might exist in Titan's thermosphere.

The presence of such a condensation layer at high altitudes could imply effects which have not yet been investigated in Titan's atmospheric modeling: a sink for heavy polyynes at high altitudes leading to an inhibition of heavy polyynes formation, and the possibility of a heterogeneous chemistry between the condensed phase and the surrounding gas.

The second region of condensation, located in the low stratosphere, is observed whatever the chosen profile or uncertainty on temperature are. This region starts around 85 km (16 mb, 135 K) down to the ground leading to a deposition of carbeneous compounds on Titan's surface.

5. Conclusion and perspectives

The UV absorption coefficient of C_6H_2 was measured on a pure gaseous sample obtained by cold distillation of a synthesized sample. The spectroscopic analysis at 233 K highlights a strong increase of the absorption coefficient for cold bands induced by a Boltzmann distribution depleting higher vibrations levels population. The new absorption coefficients will allow to constraint the contribution of C_6H_2 to the albedo of Titan below 200 nm, and less likely is the C_6H_2 detection from its forbidden transitions.

On the contrary, the reddening of the bands systems with the length of the polyynes (Grutter et al., 1998) and the linear rise of the oscillator strength could allow the detection of the allowed transition of heavier polyynes above 200 nm. Unfortunately, only the UVIS spectrometer of the Cassini-Huygens could have scan different areas of Titan's atmosphere where polyynes could be favorably present, but its maximum wavelength is 190 nm.

Concerning the IR results, we revisited the work of Delpéch et al. (1994) and demonstrate that their bands intensities were highly underestimated because of saturation effects. As we underlined above, the most intense band in the IR range investigated by CIRS, is located near 620 cm^{-1} . CIRS could detect the signature of this band in future Titan's observations, but its resolution of 0.5 cm^{-1} is too low to distinguish from one polyynes to another due to a wavelength convergence of this bending mode for higher polyynes (Shindo et al., 2001). Consequently the other IR active bending mode, standing below 300 cm^{-1} (105 cm^{-1} for C_6H_2 (Haas et al., 1994b) and 62 cm^{-1} for C_8H_2) appears as the only mean to detect those polyynes individually. Moreover, their detection could be easier since in this wavelength range Titan's thermal emission is more favorable. But the absolute intensities of those bands still need to be determined.

The rise of the oscillator strength with the number of triple bond seems to imply a quick formation of heavy polyynes, which infers a quick formation of solid particles in the hypothesis that polyynes are a chemical path leading to aerosols. From the triacetylene pressure profile in Titan's atmosphere, a condensation region in the thermosphere can exist but strongly depends on the temperature profile variations. Such absorbing layer is in agreement with an upper haze layer observed around 700 km (Smith et al., 1982). Finally this condensation layer at high altitudes could be a sink for heavy polyynes leading to an inhibition of heavy polyynes formation, and it could be the place of a heterogeneous chemistry between the condensed phase and the surrounding gas.

Acknowledgements

This work has been supported by the French National Program of Planetology (PNP) of the Institut National des

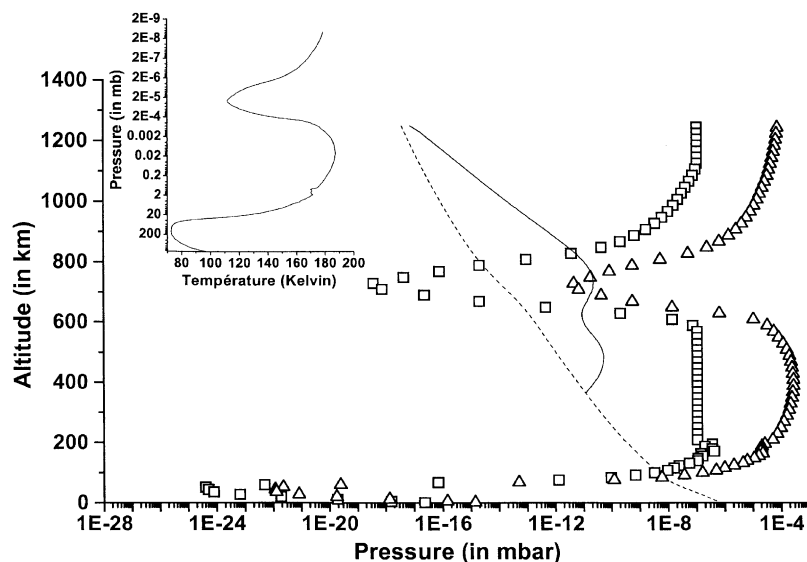


Fig. 8. The pressure profile of C_6H_2 in Titan's atmosphere according to the mole fraction calculated by Toublanc et al. (1995) (straight line) and to a constant mole fraction of 4.4×10^{-10} (dashed line). Also reported, the corresponding vapor pressure curve calculated with the recommended temperature (open squares) and the maximum temperature (open triangles) of Lellouch and Hunten (1987). Their temperature profile (pressure vs. temperature) is indicated in the diagram inserted in the upper left. Two condensation regions are possible: one in the low stratosphere (~ 100 km) and the other in the thermosphere (~ 700 km).

Sciences de l'Univers, by the French Space Agency (CNES: Centre National d'Etudes Spatiales) and by the French Exobiology Research Group (GDR Exobio). We especially thank C. Szopa and D. Coscia for their help in the GC-MS analysis of the triacetylene sample.

References

- Allen, M., Yung, Y.L., Pinto, J.P., 1980. Titan—aerosol photochemistry and variations related to the sunspot cycle. *Astrophys. J.* 242 (2), L125–L128.
- Bandy, R.E., Lakshminarayan, C., Frost, R.K., Zwier, T.S., 1992. Direct detection of C_4H_2 photochemical products: possible routes to complex hydrocarbons in planetary atmospheres. *Science* 258, 1630.
- Bandy, R.E., Lakshminarayan, C., Frost, R.K., Zwier, T.S., 1993. The ultraviolet photochemistry of diacetylene: direct detection of primary products of the metastable $C_4H_2^* + C_4H_2$ reaction. *J. Chem. Phys.* 96 (7), 5362–5374.
- Bénilan, Y., Bruston, P., Raulin, F., Courtin, R., Guillemin, J.-C., 1995. Absolute absorption coefficient of C_6H_2 in the mid-UV range at low temperature; implications for the interpretation of Titan atmospheric spectra. *Planet. Space Sci.* 43 (1/2), 83–89.
- Bénilan, Y., Andrieux, D., Khelifi, M., Bruston, P., Raulin, F., Guillemin, J.-C., Cossart-Magos, C., 1996. Temperature dependence of HC_3N , C_6H_2 , and C_4N_2 mid-UV absorption coefficients. Application to the interpretation of Titan's atmospheric spectra. *Astrophys. Space Sci.* 236 (1), 85–95.
- Bjarnov, E., Christensen, D.H., Nielsen, O.F., Augdahl, E., Kloster-Jensen, E., Rogstad, A., 1974. Vibrational spectra and force field of triacetylene. *Spectrochim. Acta* 30A, 1255–1262.
- Broadfoot, A.L., Belton, M.J., Takacs, P.Z., Sandel, B.R., Shemansky, D.E., Holberg, J.B., Ajello, J.M., Moos, H.W., Atreya, S.K., Donahue, T.M., Bertaux, J.L., Blamont, J.E., Strobel, D.F., McConnell, J.C., Goody, R., Dalgarno, A., McElroy, M.B., 1979. Extreme ultraviolet observations from Voyager 1 encounter with Jupiter. *Science* 204, 979–982.
- Bruston, P., Raulin, F., Poncet, H., 1991. A laboratory facility for mid-UV absorption spectroscopy of molecular compounds for planetary atmospheres. *J. Geophys. Res.* 96, 513–517.
- Cerceau, F., Raulin, F., Courtin, F., Gautier, D., 1985. Infrared spectra of gaseous mononitriles: applications to the atmosphere of Titan. *Icarus* 62, 207–220.
- Chassefière, E., Cabane, M., 1995. Two formation regions for Titan's hazes: indirect clues and possible synthesis mechanisms. *Planet. Space Sci.* 43 (1), 91–103.
- Coll, P., Coscia, D., Smith, N., Gazeau, M.-C., Ramirez, S.I., Cernogora, G., Israël, G., Raulin, F., 1999. Experimental laboratory simulation of Titan's atmosphere: aerosols and gas phase. *Planet. Space Sci.* 47, 1331–1340.
- de Graauw, T., Feuchtgruber, H., Bezdard, B., Drossart, P., Encrenaz, T., Beintema, D.A., Griffin, M., Heras, A., Kessler, M., Leech, K., Lellouch, E., Morris, P., Roelfsema, P.R., Roos-Serote, M., Salama, A., Vandenbussche, B., Valentijn, E.A., Davis, G.R., Naylor, D.A., 1997. First results of ISO-SWS observations of Saturn: detection of CO_2 , CH_3C_2H , C_4H_2 and tropospheric H_2O . *Astron. Astrophys.* 321, L13–L16.
- de Vanssay, E., Gazeau, M.-C., Guillemin, J.-C., Raulin, R., 1995. Experimental simulation of Titan's organic chemistry at low temperature. *Planet. Space Sci.* 43, 25–31.
- Delpech, C., Guillemin, J.C., Pailous, P., Khelifi, M., Raulin, F., 1994. Infrared spectra of triacetylene in the 4000–220 cm^{-1} region: absolute band intensity and implications for the atmosphere of Titan. *Spectrochim. Acta* 50A (6), 1095–1100.
- Fahr, A., Nayak, A., 1994. Temperature dependent ultraviolet absorption cross sections of 1,3-butadiene and butadiyne. *Chem. Phys.* 189, 725–731.
- Frost, R.K., Zavarin, G.S., Zwier, T.S., 1995. Ultraviolet photochemistry of diacetylene: metastable $C_4H_2^* + C_2H_2$ reaction in helium and nitrogen. *J. Phys. Chem.* 99 (23), 9408–9415.
- Gladstone, G.R., Allen, M., Yung, Y.L., 1996. Hydrocarbon photochemistry in the upper atmosphere of Jupiter. *Icarus* 119, 119.
- Grutter, M., Wyss, M., Fulara, J., Maier, J.P., 1998. Electronic absorption spectra of the polyacetylene chains $HC_{2n}H$, $HC_{2n}H^-$,

- and $\text{HC}_{2n-1}\text{N}^-$ ($n=6-12$) in neon matrixes. *J. Phys. Chem. A* 102, 9785–9790.
- Haas, S., Winnewisser, G., Yamada, K.M.T., Matsumara, K., Kawaguchi, K., 1994a. The high-resolution spectra of the ν_{11} band of triacetylene near 622 cm^{-1} : revised assignments for hot bands. *J. Mol. Spectrosc.* 167, 176–190.
- Haas, S., Yamada, K.M.T., Winnewisser, G., 1994b. High-resolution Fourier transform spectrum of the ν_{13} fundamental band of triacetylene in the far-infrared region. *J. Mol. Spectrosc.* 164, 445–455.
- Haink, H.-J., Jungen, M., 1979. Excited states of the polyacetylenes. Analysis of the near ultraviolet spectra of diacetylene and triacetylene. *Chem. Phys. Lett.* 61 (2), 319–322.
- Hanel, R., Conrath, B., Flasar, F.M., Kunde, V., Maguire, W., Pearl, J.C., Pirraglia, J., Samuelson, R., Herath, L., Allison, M., Cruikshank, D.P., Gautier, D., Gierasch, P.J., Horn, L., Koppany, R., Ponnampereuma, C., 1981. Infrared observations of the saturnian system from Voyager 1. *Science* 212, 192–200.
- Kloster-Jensen, E., Haink, H.-J., Christen, H., 1974. The electronic spectra of unsubstituted mono- to penta-acetylene in the gas phase and in solution in the range $1100-4000\text{ \AA}$. *Helvetica Chim. Acta* 57 (6), 1731–1743.
- Kuiper, G.P., 1944. Titan: a satellite with an atmosphere. *Astrophys. J.* 100, 378.
- Kunde, V.G., Aikin, A.C., Hanel, R.A., Jennings, D.E., Maguire, W.C., Samuelson, R.E., 1981. C_4H_2 , HC_3N and C_2N_2 in Titan's atmosphere. *Nature* 292, 686–688.
- Lara, L.M.L., E., López-Moreno, J.J., Rodrigo, R., 1996. Vertical distribution of Titan's atmospheric neutral constituents. *J. Geophys. Res.* 101(E10), 23,261–23,284.
- Laufer, A.H., Bass, A.M., 1979. Photochemistry of acetylene. Bimolecular rate constant for the formation of butadiyne and reactions of ethynyl radicals. *J. Phys. Chem.* 83 (3), 310.
- Lellouch, E., Hunten, D.M., 1987. Titan atmosphere engineering model. ESA, ESLAB (87/199).
- Maguire, W.C., Hanel, R.A., Jennings, D.E., Kunde, V.G., Samuelson, R.E., 1981. C_3H_8 and C_3H_4 in Titan's atmosphere. *Nature* 292, 683.
- Matsumara, K., Kawaguchi, K., Mc Naughton, D., Bruget, D.N., 1993. High-resolution infrared spectroscopy of the ν_5 band of triacetylene. *J. Mol. Spectrosc.* 158, 489–493.
- Mc Naughton, D., Bruget, D.N., 1991. The high-resolution infrared spectrum of triacetylene. *J. Mol. Spectrosc.* 150, 620–634.
- Okabe, H., 1983. Photochemistry of acetylene at 1849 \AA . *J. Chem. Phys.* 78 (3), 1312–1317.
- Ridley, J., Zerner, M., 1973. An intermediate neglect of differential overlap technique for spectroscopy: pyrrole and the azines. *Theoret. Chim. Acta* 32 (2), 111–134.
- Shindo, F., Bénilan, Y., Chaquin, P., Guillemin, J.-C., Jolly, A., Raulin, F., 2001. IR spectrum of C_8H_2 : integrated band intensities and some observational implications. *J. Mol. Spectrosc.* 210 (2), 191–195.
- Smith, N., 1999. Sensibilité des modèles théoriques de l'atmosphère de Titan aux incertitudes sur la photochimie des hydrocarbures simples. Université Paris 12 Val de Marne, Créteil, 1999.
- Smith, G.R., Strobel, D.F., Broadfoot, B.R., Sandel, B.R., Shemansky, D.E., Holberg, J.B., 1982. Titan's upper atmosphere-composition and temperature from the EUV solar occultation results. *J. Geophys. Res.* 87, 1351.
- Smith, P.L., Yoshino, K., Parkinson, W.H., Ito, K., Stark, G., 1991. High-resolution, VUV (147–201 nm) photoabsorption cross sections for C_2H_2 at 195 and 295 K. *J. Geophys. Res.* 96, 17529–17533.
- Strobel, D.F., 1982. Chemistry and evolution of Titan's atmosphere. *Planet. Space Sci.* 30 (8), 839–848.
- Toublanc, D., Parisot, J.P., Brillet, J., Gautier, D., Raulin, F., McKay, C.P., 1995. Photochemical modeling of Titan's atmosphere. *Icarus* 113, 2–26.
- Vervack, R.J., Sandel, B.R., Strobel, D.F., 1999. First results from a reanalysis of the Voyager 1 ultraviolet spectrometer solar occultations by Titan. *Icarus*, submitted for publication.
- Yung, Y.L., Allen, M., Pinto, J.P., 1984. Photochemistry of the atmosphere of Titan: comparison between model and observations. *Astrophys. J. Suppl. Ser.* 55, 465–506.